

# Chaos in Wall Following Robots

Steve Meisburger\* and Alfred Hubler†

*Santa Fe Institute, 1399 Hyde Park Road, New Mexico 87501, USA*

(Dated: September 6, 2006)

We study generalized wall following behavior of mobile robots using numerical simulations. We find that the dynamics are chaotic over a range of parameter values. In addition, we propose a theory of wall following where the robot-wall combination can be treated as a pendulum-like nonlinear oscillator, driven by perturbations in the environment. We compute the dominant Lyapunov exponent for a robot following a periodic undulating wall and the divergence of neighboring trajectories of wall following robots in a maze.

PACS numbers: 05.45.Ac, 05.45.Gg, 05.45.Pq

This paper addresses a need for increased understanding of the origins of complex behavior in mobile robots. Recent research has reported chaos from time series analysis of a mobile robot running an obstacle avoidance program [1], though no apparent effort was made to understand this behavior theoretically. Recent efforts to apply the theory of dynamical systems to robotics include the study of chaos in robotic arms [2, 3], legged robots [4], and neural controllers [5]. In addition, applications for chaotic robots have been proposed, including security patrol and cleaning [6]. Their research included the design and testing of a chaotic robot controller which integrates a known chaotic differential equation [6]. However, if chaos is somehow intrinsic to robot dynamics, this would obviate the need for a chaotic controller.

We study chaotic behavior of a mobile robot following a wall in order to demonstrate that such behavior can be produced without the need for internal memory or sophisticated control algorithms. Wall following behavior (thigmotaxis) has been examined in insects [7] and mice [8]. It has also been implemented as an elementary behavior in video game AI [9] and in mobile robots [10]. We analyze this behavior because it can be easily achieved with continuous, autonomous control equations facilitating comparison with known chaotic systems. First, we propose a generalized model of a wall following robot with a single distance sensor. We perform a parameter sweep over the sensor field of view for a robot following a sinusoidal wall and find a transition to chaos by period doubling bifurcations, confirmed by measurements of the largest Lyapunov exponent. Next, we derive the isomorphism of the differential equations for a robot following a flat wall and the simple pendulum, a nonlinear oscillator. We propose an explanation for the chaotic behavior of our wall following robot where the limited field of view

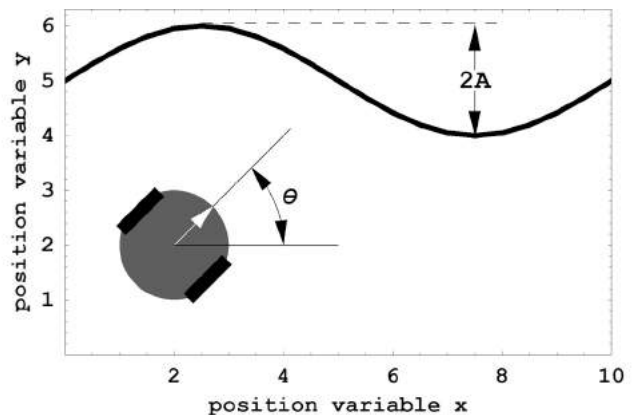


FIG. 1: Model of a robot where the state is completely specified by the position variables  $x$ ,  $y$ , and  $\theta$ . Also shown is a sinusoidal wall used for the chaos study, with amplitude  $A = 1$  and period  $P = 10$ . The environment has periodic boundary conditions such that the  $(y, \theta)$  planes  $x = 0$  and  $x = 10$  are equivalent.

is similar to damping, and variations in the environment drive the nonlinear oscillator into the chaotic regime.

In this investigation we consider the dynamics of a two-wheel mobile robot (fig.1). Constraints on robot motion arise because it must travel in the direction that the wheels are pointing. In reality, robots are subject to constraints on acceleration due to their mass and the nonideal operation of motors and wheels. However, these effects can be minimized by keeping the robot at a reasonable speed. The following is known as the low speed approximation [6, 11].

$$\begin{aligned}\dot{x} &= v \cos \theta \\ \dot{y} &= v \sin \theta \\ \dot{\theta} &= \omega\end{aligned}\tag{1}$$

where  $x$  and  $y$  are the Cartesian coordinates of the robot position in the plane, and  $\theta$  is the angle of the robot measured counter-clockwise from the  $x$ -axis. The control parameters  $v$  and  $\omega$  correspond to the speed and rotational rate of the robot. They are related to the left

\*Current address: Department of Physics and Astronomy, Carleton College, One North College Street, Northfield, Minnesota 55057; Electronic address: meisburs@carleton.edu

†Permanent address: Center for Complex Systems Research, Department of Physics, 1110 W Green Street, University of Illinois at Urbana-Champaign, Illinois 61801; Electronic address: a-hubler@uiuc.edu

and right wheel speeds,  $u_L$  and  $u_R$  respectively, by

$$\begin{aligned} u_R &= \frac{2v + l\omega}{2r} \\ u_L &= \frac{2v - l\omega}{2r} \end{aligned} \quad (2)$$

where  $r$  is the wheel radius and  $l$  is the distance between the right and left wheels. Due to the linearity of eq. 2,  $v$  and  $\omega$  are equivalent to  $u_L$  and  $u_R$  as control parameters. We use the former because they are independent of robot geometry ( $r$  and  $l$ ).

A wall following algorithm attempts to maintain a constant distance from a wall while moving along it. Intuitively, the robot must turn toward the wall if beyond the target distance  $D$ , and away from the wall if too close. We propose a generalized wall following algorithm where the speed,  $v$ , is held constant while the robot sets its rotational speed,  $\omega$ , proportional to the deviation from the target wall distance,  $D$ . In addition, we require that the robot's forward-facing distance sensor has a finite range and field of view (fig. 2). Our control algorithm for following a wall on the robot's left is as follows:

$$\begin{aligned} v &= 1 \\ \omega &= \sigma(x, y, \theta) - D \end{aligned} \quad (3)$$

where  $\sigma$  is the distance to the nearest object seen by the sensor, a function that depends in general on the robot's position and angle. It is assumed that length and time are in dimensionless units.

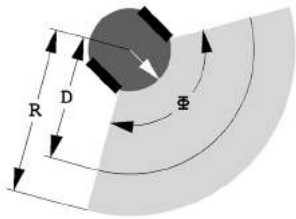


FIG. 2: Diagram showing sensor geometry for wall following robot. The sensor continuously reports the closest object within its field of view,  $\Phi$ , and range,  $R$ . Also shown is the target following distance,  $D$ .

We simulate a robot following a wall by combining equations 1 and 3 and solving them numerically using a fourth-order Runge-Kutta algorithm with a fixed timestep of 0.01. The robot was placed in an environment consisting of a sinusoidal wall given by  $y = \sin(\pi x/5) + 5$ .

Calculating the distance between the robot and the wall involves finding the solution of a transcendental equation. For the sake of efficiency, the wall was discretized by dividing the sinusoid into twenty line segments per period. Distances and intersections were then computed exactly using standard geometry. Because the wall repeats every 10 steps in the  $x$ -direction, the use of periodic boundary conditions was natural. We calculated piercings of the plane  $x = 0 = 10$  by finding the

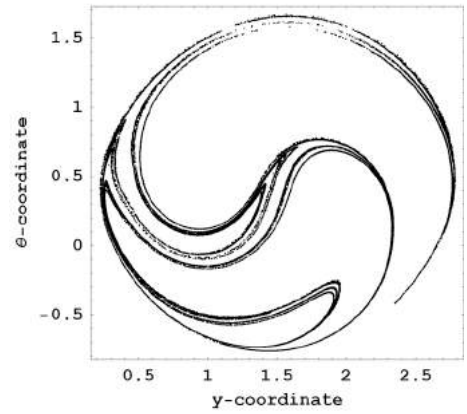


FIG. 3: Poincaré map computed for  $R = 4$ ,  $D = 3$ , and  $\Phi = 5\pi/3$ . 68,000 points are shown.

intersection of a line between points on either side of the plane. This was adequate because the resulting Poincaré section was used only for visualization of the attractor.

After an informal sweep through parameter values, it was found that the wall following behavior appeared chaotic for a sensor range of 4.0, a target following distance of 3.0, and a field of view greater than  $3\pi/2$  (fig.3).

The largest Lyapunov exponent was calculated using a time  $T=1$  mapping according to the method of Benettin et al. [12]. First, the system was set to the initial condition  $(x, y, \theta) = (0, 1, 0)$  and allowed to run for 20,000 time units to assure that the system had settled into the attractor. Then, a neighboring trajectory was initialized alongside the first, set at a distance of  $\sqrt{3} * 10^{-6}$  away ( $10^{-6}$  in the  $x, y$  and  $\theta$  directions). For a chaotic system, the largest Lyapunov exponent dominates, and the distance between neighboring trajectories grows ex-

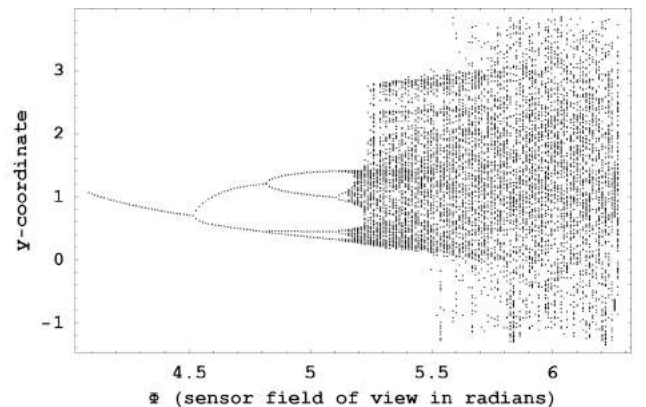


FIG. 4: Bifurcation diagram showing the transition to chaos by period doubling. Sensor range and field of view were held constant at  $R = 4$  and  $D = 3$ , respectively, while field of view was increased from  $\Phi = 13\pi/10$  to  $2\pi$  in steps of  $\pi/240$ . Each vertical band consists of 100 consecutive piercing of the  $x = 0 = 10$  plane.

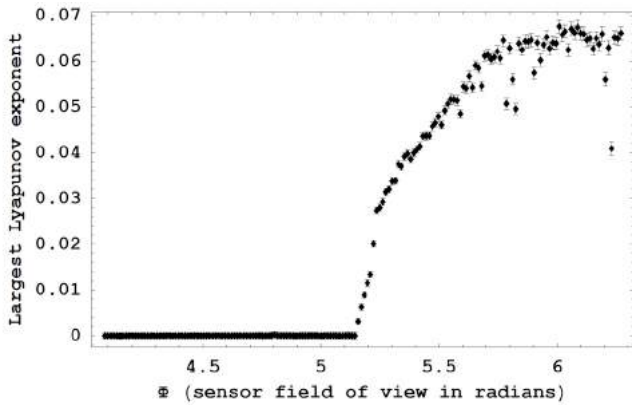


FIG. 5: Numerical estimates of the largest Lyapunov exponent for parameter values  $R = 4$ ,  $D = 3$ , and  $\Phi$  between  $13\pi/10$  and  $2\pi$  in steps of  $\pi/240$ . A Lyapunov exponent greater than zero signifies chaos. Each point represents the average over 200,000 measurements of the local divergence of neighboring trajectories. Error bars show the standard deviation of the mean.

ponentially. Therefore, the vector between the neighboring trajectories was renormalized every time unit, after recording the growth ratio of the vector. The simulation was allowed to run approximately 64,000 time units, and the Lyapunov exponent was computed as the average of the natural logarithm of the growth ratios.

The simulation was repeated 168 times, varying the sensor field of view from  $13\pi/10$  to  $2\pi$  in steps of  $\pi/240$ . By collapsing the Poincaré sections onto the  $y$ -axis we create a bifurcation diagram (fig. 4), where it can be seen that the transition to chaos occurs by period-doubling.

A plot of our best estimates of the largest Lyapunov exponent over the same parameter range confirms onset of chaos and persistence for sensor field of view between  $197\pi/120$  and  $2\pi$  (fig. 5).

The chaotic motion of a robot following a wall can be explained by the similarity of the system to the simple pendulum. Consider a robot with an "ideal" distance sensor ( $R = \infty$ ,  $\Phi = 2\pi$ ), following a flat wall given by the equation ( $y = W$ ). Under these conditions, the sensor measures the difference between the wall's  $y$ -coordinate and the robot's  $y$ -coordinate, enabling us to write an explicit formula for the sensor function:  $\sigma(y) = W - y$ . Inserting this into the constraint equation 1, one obtains the coupled differential equations

$$\dot{y} = v \sin \theta \quad (4)$$

$$\dot{\theta} = (W - y) - D \quad (5)$$

Taking the time derivative of eq. 5 and substituting in eq. 4, one obtains the second-order equation in  $\theta$

$$\ddot{\theta} = -v \sin \theta \quad (6)$$

This is exactly the equation for a simple pendulum where  $\theta$  is the angle of the pendulum measured from the downward vertical. With the addition of viscous damping and periodic forcing, the pendulum has well-known chaotic behavior [13]. In our case, the robotic equivalent of viscous damping is the limitation on sensor field of view, which introduces a  $\dot{\theta}$  dependence in eq. 6. The periodic sinusoidal wall provides the driving force necessary for chaotic behavior.

- 
- [1] U. Nehmzow. Quantitative analysis of robot-environment interaction: towards "scientific mobile robotics". *Robotics and Autonomous Systems*, 44(1):55–68, 2003.
- [2] H. J. Cao, X. B. Chi, and G. R. Chen. Suppressing or inducing chaos in a model of robot arms and mechanical manipulators. *Journal of Sound and Vibration*, 271(3-5):705–724, 2004.
- [3] S. Lankalapalli and A. Ghosal. Chaos in robot control equations. *International Journal of Bifurcation and Chaos*, 7(3):707–720, 1997.
- [4] S. Aoi and K. Tsuchiya. Bifurcation and chaos of a simple walking model driven by a rhythmic signal. *International Journal of Non-Linear Mechanics*, 41(3):438–446, 2006.
- [5] M. Islam and K. Murase. Chaotic dynamics of a behavior-based miniature mobile robot: effects of environment and control structure. *Neural Networks*, 18(2):123–144, 2005.
- [6] Y. Nakamura and A. Sekiguchi. The chaotic mobile robot. *IEEE Transactions on Robotics and Automation*, 17(6):898–904, 2001.
- [7] J. M. Camhi and E. N. Johnson. High-frequency steering maneuvers mediated by tactile cues: Antennal wall-following by the cockroach. *Journal of Experimental Biology*, 202(5):631–643, 1999.
- [8] S. B. M. Kvist and R. K. Selander. Maze-running and thigmotaxis in mice - applicability of models across the sexes. *Scandinavian Journal of Psychology*, 33(4):378–384, 1992.
- [9] C. W. Reynolds. Steering behaviors for autonomous characters. *proc. of Game Developers Conference 1999*, pages 763–782, 1999.
- [10] R. Carelli and E. O. Freire. Corridor navigation and wall-following stable control for sonar-based mobile robots. *Robotics and Autonomous Systems*, 45(3-4):235–247, 2003.
- [11] S.M. Lavalle. *Planning algorithms*. Cambridge University Press, 2006.
- [12] G. Benettin, L. Galgani, A. Giorgilli, and J.-M. Strelcyn. Lyapunov characteristic exponents for smooth dynamical systems and for hamiltonian systems - a method for computing all of them. ii - numerical application. *Meccanica*, 15:9–30, Mar 1980.
- [13] D. D’Humieres, M. R. Beasley, B. A. Huberman, and A. Libchaber. Chaotic states and routes to chaos in the forced pendulum. *Phys. Rev. A*, 26(6):3483–3496, Dec 1982.